Correlation between microstructure and creep behaviour in liquid-phase-sintered α-silicon carbide

M. Castillo-Rodríguez, A. Muñoz, A. Domínguez-Rodríguez

Departamento de Física de la Materia Condensada. Universidad de Sevilla.
Apartado 1065. 41080-Sevilla. Spain

The influence that the (Argon atmosphere and) sintering time (1 and 7 hours), in Argon atmosphere, has(ve) on microstructure evolution in α-SiC sintered at 1950 ºC with Y_2O_3-Al_2O_3 (10 % weight) as liquid phase (LPS-α-SiC) and on its mechanical properties at high temperature was investigated.

The (samples sintered in Ar had an elongated-grain microstructure with a) density of the samples decreasing from 98.8 % to 94.9 % of the theoretical value and the grain size increasing from 0.64 to 1.61 μm (as) when the sintering time increases(d) from 1 to 7 hours, taking place a very important elongating in a part of the grains.

The compression creep behaviour has been studied at reduced atmosphere, at temperature between 1450 and 1625 ºC and stresses between 25 and 450 MPa, being the strain rate between $4.2 \cdot 10^{-8}$ and $1.5 \cdot 10^{-6}$ s^{-1}. The creep parameters (stress exponent n and the activation energy Q) has been determined, obtaining(ed) for n values between 2.4 ± 0.1 and 4.5±0.2 and Q=680±35 $kJ.mol^{-1}$ in samples sintered during 1 hour and n between 1.2±0.1 and 2.4±0.1 and Q=710±90 $kJ.mol^{-1}$ for samples sintered during 7 hours. The correlation between these results and the microstructure indicates that grain boundary sliding and the glide and climb of dislocation accommodated both by the bulk diffusion, can be two independent deformation mechanism operating in these LPS-α-SiC.

(During mechanical tests, a loss of intergranular phase takes place in a region, between 50 and 150 μm thick, close to the surface of the samples — the effect being more important in the samples sintered in Ar.)

At the temperature of the tests there are solid state reactions between SiC and the sintering additives producing volatile products which are responsible for the (change the microstructure by) increases(ing the) of porosity and of the decrease of intergranular phase in the samples during the thermal treatment to the mechanical test temperature. These effects are more important in regions near the surface of the samples. These structural changes are not consequence of the process of deformation but rather they are due to the lingering thermal treatment of the material during the creep and they cease after having lapsed the first two or three days of mechanical testing, reaching the material a stable microstructure. (Como afecta esto a las prop. Mecán?)

(Whereas the stress exponent change with the stress and the annealing time, the activation energy remains almost constant regardless the creep parameters (stress, T and annealing time). These parameters have been correlated with the microstructure in order to determine the mechanism controlling the plasticity of these LPS-α-SiC.)

Keywords: liquid-phase sintered(ing); α-SiC; creep; microstructure; mechanical properties.

1. Introduction

Amongst the structural materials to be used in industry in severer conditions, SiC has been one of the most widely studied in the last few decades, due to its remarkable mechanical properties at high as well as at low temperatures, its low density, and its excellent resistance to corrosion and good thermal shock. However, it is difficult to obtain fully dense materials

due to the covalent bonding between Si and C, the low diffusion coefficient of the two species and the high energy of the grain boundaries, being necessary temperature and sintering pressure very high. It has been necessary to develop sintering techniques to reduce temperatures and stresses using liquid phase aids (LPS) which melt at low temperatures allowing the material densification and joining the SiC grains.

In much of the industrial applications, the material is submitted to high mechanical or thermal stresses, as (a) consequence of thermal gradient, for what the (so the ac) knowledge of the high temperature mechanical properties is very important to control such applications.

Although in the last decades, its has been published several studies related with the high temperature creep behavior of SiC[1-9], there are some scatter in the results due to that the mechanisms controlling plasticity strongly depend on the microstructure and this is fundamentally function of the obtaining method and also of other parameters like the grain size, the densification degree, impurities and, in the LPS-SiC, of (this in turn on) the amount and type of the liquid phase used during sintering, type of starting powder, temperature, time, and sintering atmosphere. In this regard, Lane et al.[1] using C (0.5 %-wt), B (0.42 %-wt) and small amount of other impurities, obtained a fully-dense α-SiC at 2100 ºC with a grain size of 3.7 μm. They suggest that the mechanism controlling plasticity is grain boundary sliding (GBS) accommodated by bulk diffusion of the atomic (two) species for temperature below 1650 ºC. At higher temperatures, they find that the activity of dislocations contributes from a significant way to the mechanisms controlling plasticity. (is mainly due to the activity of dislocations). Nixon et al.[2] using the same type of α-SiC but with different grain sizes, obtained the same results that Lane et al.[1], being the contribution of the dislocations to the mechanisms controlling plasticity a function of the grain size.

Backhaus-Ricoult et al[3], studied the mechanical properties of two SiC obtained by hot isostatic press (HIP) at 2000 ºC and 2 kbar; one of them without impurities and the other with impurities of B, Si, Fe, O and C with a concentration below 2000 p.p.m. They suggest GBS as the mechanism controlling plasticity accommodated by grain boundary diffusion and cavitation for stresses below 500 MPa. At higher stresses, grain boundaries are not longer obstacles to the movement of dislocations through them, being then the movement of dislocations the mechanism controlling the plasticity. On the other hand, they find an increment in the speed of deformation like consequence of the presence of the additions.

Hamminger et al.[4], performed compressive tests at a constant load on several SiC doped with Al and C and B and C at temperatures between 1470 and 1660 ºC and stresses between 100 and 190 MPa. They concluded that the bulk diffusion processes are the mechanism controlling plasticity.

Jou et al.[5] using Al_2OC (10 %-wt) as a liquid phase aid, obtained a SiC at 1875 ºC and with a grain size of 2 μm. Using compressive tests at a constant load, they concluded that at temperatures between 1500 and 1650 ºC, the deformation is controlled simultaneously by bulk diffusion processes and dislocation activity.

Gallardo-López et al.[6] studied the creep behavior of an LPS-α-SiC sintered with a small amount of liquid phase — less than 2 %-vol Y_2O_3 and Al_2O_3 — and with a grain size of 1.2 μm deformed at temperatures between 1575 and 1700 °C and with stresses between 90 and 500 MPa. The mechanisms of deformation proposed by these authors are the GBS accommodated by volume diffusion and the dislocations activity, acting in a simultaneous way. (The deformation is due to GBS controlled simultaneously by volume diffusion of point defects and dislocation activity.)

For a SiC with 10 to 12 %-vol of free Si obtained by reaction of the Si in gassy state with (between a partial pression of Si in) a porous preform of SiC with free C, Carter et al[7], suggest that the dislocation activity is the mechanism controlling plasticity of these materials at temperatures between 1575 and 1650 ºC and stresses between 110 and 220 MPa.

Muñoz el al.[8] and Martinez-Fernandez el al.[9] studied the high temperature mechanical behavior of a SiC formed by the reactive infiltration into microporous carbon performs of molten silicon (9 and 20 %-vol free Si) or silicon-(9 % vol)niobium alloy (9 %-vol free Si+$NbSi_2$). (into microporous carbon performs.) The mechanical tests were performed in compression at cross-head speed or load constant at temperature between 1300 and 1350 ºC. The SiC grains not undergo significant plastic deformation and the mechanism controlling plasticity is due to the movement and redistribution of the viscous grain boundary remainder phase, in such a way that the strain rate decreases to zero when the SiC grains become in contact.

The objective of the present work was to correlate the microstructure and mechanical behavior of a LPS-α-SiC, with Y_2O_3 and Al_2O_3 as liquid phase (10 %-wt), and sintered in Argon atmosphere for two different process times, 1 and 7 hours. The mechanical tests were performed at a constant load, and the microstructure before and after deformation was determined by scanning electron microscopy (SEM). The results are discussed in the base of the ones found in the literature for SiC fabricated with different techniques.

2. Experimental techniques

The powder used in this work was composed of 90% α-SiC and 10% Y_2O_3 and Al_2O_3 as intergranular phase in the ratio 3/5 to get yttrium aluminium garnet $Y_3Al_5O_{12}$ (YAG). The powders were sintered in the Department of Metallurgy and Material Science Engineering, Institute of Materials Science, University of Connecticut, USA, at 1950 ºC in Argon atmosphere for two times, 1 and 7 hours, and the densities of the materials were 98.8 ± 0.6 % and 94.9 ± 1.0 % respectively. For more details see references[10,11].

The microstructure characteristics — grain size and morphology, pore distribution, and damage after high temperature tests — were determined using a Philips Model XL-30 scanning electron microscope (SEM; electron microscopy service, University of Seville, Spain) operating at 30 kV using backscattered and secondary electrons. Prior to observation, the samples were polished with diamond paste of grain size down to 1 μm, and plasma (CF_4 and O_2 in the ratio 1:6) etched for 2 hours (Plasma Asher K1050X, Emitech). In some cases, the samples were sputter-coated with gold to avoid charge effects during observation. The morphological characteristics were determined using a Videoplan image analyzer (Videoplan MOP 30, Kontron Electronik).

Specimens of 5×2.5×2.5 mm of the two materials were machined out and polished to a 3 μm finish. Uniaxial compression tests were performed at constant load in a prototype creep machine, equipped with SiC as pushing rods, with the top pushing rod fixed and mobile the bottom one. The heating elements are (in) of wolfram able to go up to 1900 ºC, and the thermocouple is W–5 % Re / W–26 % Re. For more details see reference[12]. The creep tests have been performed in Argon atmosphere, at temperatures between 1550 and 1625 ºC and with stresses between 25 and 450 MPa. To get the work atmosphere they have been carried out, to ambient temperature, several vacuum cycles (10^{-6} Pa) followed by introduction of Argon. These cycles repeat to 500 ºC to eliminate the products of the possible degasify of the elements of the interior of the work camera. The square face of the specimen (2.5×2.5 mm) was placed normal to the loading axis and the specimens were sandwiched between two solid-state-sintered SiC platelets in order to avoid damage to the pushing rods.

3. Results and discussion

3.1. Microstructure characterization

Figure 1 is formed by typical SEM micrographs of the samples used in the present work. One observes that the SiC grains (dark contrast) are surrounded by the intergranular phase (light contrast). Also, the intergranular phase is homogeneously distributed (Figs 1a and 1c), and there exists a small amount of residual porosity, more pronounced in the samples sintered (annealed) during 7 hours (Figs 1b and 1d). This porosity is consistent with the density of the samples as measured by Archimedes' method. Table 1 lists the values of the density compared with the theoretical value of 3.310 ± 0.002 g/cm^3. One observes that, consistent with the observed increase in porosity (Fig. 1), the density of Ar-LPS-α-SiC decreased from 98.8 % to 94.9 % of the theoretical value as the sintering time increased from 1 to 7 hours.

(Fig. 1)

In figures 1b and 1d can also be observed that the intergranular phases (YAG) are located at the triple points, forming pockets. (Probably, a thin layer of glassy phase, unobserved under SEM, surrounds the SiC grains.) Although a thin layer of glassy phase has not been detected by SEM, probably it remains surrounding the SiC grains. This layer has been observed by Nagaro et al.[9] by HRTEM in liquid-phase-sintered SiC with similar amounts of sintering additives (9 %-wt Al_2O_3-Y_2O_3). The samples annealed during 7 hours present few big grains with an important increased of the aspect ratio. As a consequence, for the longest sintering time samples, both the grain size and the aspect ratio presented a bimodal distribution. It can be also observed the core-shell substructure within the SiC grains. This is indicative of grain growth occurring by the smaller grains dissolving in the liquid (glassy) phase, followed by precipitation of C and Si atoms onto the largest grains. The core (dark contrast inside the grains) represents the original growing grains, and the shell represents the newly deposited material[13,14]. The difference in contrast is because the shell contains traces of Y, Al, and O that come from the glassy phase. This substructure is more difficult to distinguish in the largest grains because the relative smallness of the original grain compared to the final grain makes it less likely to be present in the cross section.

The anisotropic evolution of a few grains for the longer sintering time (7 hours) can be understood as the result of the presence of a certain amount of β phase seeds in the α-SiC starting powders. At the sintering temperature, the β→α phase transformation takes place within these grains, resulting in grains with a composite β/α. The silicon and carbon species dissolve in the liquid and re-precipitate as α-SiC onto α-SiC regions in order to minimize the free energy of the system, thereby leading to the grains having a much higher aspect ratio which increases with annealing time. This transformation process is widely documented in the literature[14-18] and is used to obtain a SiC with a predetermined microstructure. The aspect ratio of the highly elongated grains hinders intergranular phase redistribution, and consequently it contributes to the increment of (the) porosity of the samples when the (increases with) sintering time increases. Indeed, for the 7-hour annealed samples, the main porosity is located near the largest grains (Fig. 1d).

The morphological parameters of the grains for the two types of sample were determined from SEM micrographs of different parts of the samples, using between 350 and 450 grains in each case. Together with the grain size (equivalent planar diameter, $d=(4\cdot\text{area}/\pi)^{1/2}$) of the materials studied, other parameters such as the form factor ($F=4\pi\cdot\text{area}/\text{perimeter}^2$) and the aspect ratio F_{asp}, defined as the ratio between the maximum length and the minimum width taken perpendicular to the length in the planar section of the grains, were measured. Table 1 gives the means and standard deviations of the morphological parameters, with all the parameters assumed to be normally distributed, together with the densities of both types of (the two) samples.

Tabla 1

3.2. Creep tests

Figure 2 shows a typical creep curve of a sample annealed for 7 hours. The test has been performed at temperature between 1600 and 1625 ºC and for stresses between 157 and 318 MPa. The strain rates were in between (5) $4.4 \cdot 10^{-8}$ and $3.2 \cdot 10^{-7}$ s^{-1}. For each experimental conditions (temperature and stress), a steady state is obtained characterized by a constant strain rate, after a regimen transitory initial, in which the strain rate changes quickly. (after less than 1 % of deformation except for the initial experimental conditions, probably due to the setting in place of the sample, the pads and the pushing rods.) During test, stress or temperature(s) changes were made, to determine the creep behaviour with these parameters.

(Fig. 2)

The creep curves have been analyzed using the phenomenological typical creep equation:

$$\dot{\varepsilon} = A \frac{\sigma^n}{d^p} \exp\left(-\frac{Q}{kT}\right) \qquad [1]$$

where $\dot{\varepsilon}$ is the steady strain rate, σ is the applied stress, d is the main grain size, k the Boltzmann constant and T the absolute temperature; A is a stress and temperature independent term including the dependence of the strain rate on the microstructural features of the material (grain morphology, composition and amount of glassy phases, physical properties of these, etc.). The parameters n, p and $Q^{(app)}$ (named generically creep parameters) are, respectively, the stress and the grain size exponents and the apparent activation energy for creep. In this study, we have determined only n and Q, because to determine p, we need samples with the same characteristic but with different grain size; in our case, the samples annealed at 1 and 7 hours, not only changes the grain size but also other morphological parameters, like (as) it was shown in Table 1. Figure 2 shows, together with the experimental conditions, the values of n and Q obtained for this test.

Figure 3 is a steady state strain rate vs. stress logarithmic plots for the sample sintered during (annealed) 1 hour and deformed at 1550 ºC, 1600 ºC and 1625 ºC, whereas Figure 4 corresponds at the sample sintered during (annealed) 7 hours and deformed at 1580 ºC, 1600 ºC and 1625 ºC. It can be observed that all points aligned in a straight line, indicating that during the creep test for a given temperature, the microstructure remains constant and that the stress exponent is also constant in the range of stress considered. The strain rates obtained for these two types of samples, are in between $4.2 \cdot 10^{-8}$ and $1.5 \cdot 10^{-6}$ s^{-1} for the samples annealed 1 hour and between $4.3 \cdot 10^{-8}$ and $3.2 \cdot 10^{-7}$ s^{-1} for the samples annealed 7 hours. For a same temperature and stress, the strain rate of the sample annealed 1 hour is at least one order of magnitude higher than for the sample annealed 7 hours. The different microstructure of the samples, with large grain size and aspect ratio developed during the longer sintered time can justified the different strain rate found.

(Fig. 3 y 4)

The slope of these plots in figures 3 and 4 correspond to the n values for the (two samples and the) different temperatures used in both types of samples. For samples sintered during 1 hour, the value of n measured was $n=2.4 \pm 0.1$ for the higher temperatures (1600-1625 ºC) and lower stresses (25-140 MPa). For the lower temperature (1550 ºC) and higher stresses (200-450 MPa) the value was $n=4.5 \pm 0.2$. In the case of samples sintered during 7 hours, the value was $n = 1.2 \pm 0.1$ for T= 1625 ºC and stresses between 60 and 200 MPa. For

lower temperatures (1600 and 1580 ºC) and higher stresses (160-400 MPa), the value was $n=2.4 \pm 0.2$. The stress exponent determined by changing the load at a fixed temperature (Fig. 2) or by a log-log plot of the steady state creep rate versus stress (Figs. 3 and 4) are in very good agreement, indicating that not significant changes in the microstructure occur during deformation.

For both types of samples, the values of the activation energy Q obtained in the different jumps of temperature among the three used temperatures are very close and within the experimental error it can be considered the same. (In the case of the activation energy,) The values obtained are $Q=685 \pm 35$ kJ·mol^{-1} and $Q=710 \pm 90$ kJ·mol^{-1} for samples annealed 1 and 7 hours respectively independently of (regardless) the experimental conditions. (The values obtained in both type of samples are very close and within the experimental error it can be considered the same.) Table 2 show(s) the value of tests parameters and the different values of n and Q obtained for the two types of samples.

(Tabla 2)

The values of Q obtained in this work are in good agreement with the values found in the literature for the bulk diffusion of C (715–840 kJ·mol^{-1})[19,20] and Si (695–910 kJ·mol^{-1})[21,22] in SiC, indicating that the mechanism controlling plasticity are governed by diffusion(al) processes inside the grains. Because the diffusion coefficient of Si is, at least one order of magnitude lower than this of C, it must be the bulk diffusion of Si who controls the plasticity. These data have been obtained in α–SiC single crystals pure and doped with N (620 p.p.m.) and in β–SiC polycrystals doped with Cu (60 p.p.m.).

On the other hand, our Q and n values are in agreement with the ones found in the literature[1-7] for SiC sintered with different techniques. Table 3 is a compilation of the results found in the literature for the creep of SiC.

(Tabla 3)

(3.3. Microstructure characterization after deformation)

The morphological parameters obtained by SEM for the samples deformed, indicate that the (grain) size and form of the grains (factor) remained unchanged after of the deformation. Thus, for samples (annealed) sintered during 1 hour and deformed at 1625 ºC, it was measured $\bar{d} = 0.72 \pm 0.02$ μm, $\sigma_d = 0.35 \pm 0.01$ μm, $\bar{F} = 0.82 \pm 0.01$, $\sigma_F = 0.09 \pm 0.01$, $\bar{F}_{asp} = 1.57 \pm 0.02$ y $\sigma_{Fasp} = 0.39 \pm 0.01$; values very close to the ones measured in similar samples prior to deformation (Table 1). The observed microstructure morphology indicates that grain boundary sliding is the main deformation mechanism in this system; The value obtained for Q suggests that the accommodation process is the bulk diffusion of Si, (being the mechanism) This mechanism of deformation has been broadly proposed in the literature to explain the creep behaviour in SiC prepared with different techniques[1-7]. The different models accounted for this mechanism predict a stress exponent equal to 1[23-24]; however, the measured stress exponent is larger than one, in accord with previous studies in polycrystalline SiC, and not in agreement with predictions of models. Therefore, another mechanism with similar activation energy but larger stress exponent must also be operating in parallel with GBS.

As it can be seen in Table 2, the stress exponent increases when the applied stress increases and values as high as 4.5 can be measured for the lower temperature and the higher stresses. This fact together with the constant activation energy regardless the applied stress, suggest that the glide and climb of dislocation can be an independent deformation mechanism in addition to GBS. When the climb of dislocations is responsible for deformation, being the

climb of dislocation controlled by the bulk diffusion of point defects, stress exponent between 3 and 10 can be found in the literature. This mechanism is normally called power-law creep (PLC) and a review of the different models can be found in[25]. According with the results of the mechanical tests this contribution should be bigger in the samples sintered during 1 hour that in the sintered during 7 hours, possibly due to its different microstructure.

This combination between GBS (n=1) and PLC (n≥3) has been suggested by several authors. Thus, Lane et al[1] observed by TEM a high density of dislocations homogeneously distributed in the grains, faults, glide bands and climb of dislocations justifying the stress exponent between 1.44 and 1.71 found at temperatures between 1550 and 1750 ºC as a consequence of the combination of two independent mechanisms, GBS accommodated by bulk diffusion and high dislocation activity controlled by climb. The same explanation has been postulated by Nixon el al.[2] to justified n values between 1.4 and 2.5 found at temperatures T>1650 ºC and by Jou et al.[5] to justified n=1.74 found (for) at temperature of 1575 ºC and stresses between 38 and 200 MPa. (que temperature).

Backhaus-Ricoult et al.[3] found a high density of dislocations and values of n between 3.5 and 4 when the materials are deformed a stresses higher than 500 MPa. They assume that at this high stresses, the dislocations can cross grain boundaries because these defects are not longer obstacles for the movement of dislocations, being this the dominant deformation mechanism at these experimental conditions.

Gallardo-Lopez et al.[6] in a liquid phase sintered SiC but with smaller amount of intergranular phase (lower than 2 %-vol) than the materials used in this work, found a stress exponent of 1.6 when deformed at temperature between 1575 and 1700 ºC and stresses between 90 and 500 MPa.. The crept samples showed the presence of dislocation activity, with glide and climb of dislocations forming tangles. They concluded that the creep mechanisms operating are GBS accommodated by lattice diffusion and climb-controlled dislocation glide operating in parallel.

3.3. Microstructure characterization after deformation

Although the morphological parameters do not change significantly during deformation, there is a significant increases of density of cavities and voids in sample deformed compared with the as-received material, which increase when approach to the surface. At the same time, it can be observed a decrease of the intergranular phases, more important in regions close to the surface. (In this area,) The remainder intergranular phase is located primarily in the voids formed between SiC grains during the tests (deformation between SiC grains). Figure 5 shows the main features outlined and it is a composition of four micrographs. Figures 5a and 5b correspond to a sample annealed for 1 hour and deformed at 1625 ºC. Figure 5a corresponds to a region close to the surface whereas figure 5b corresponds to a region in the middle of the sample. Figures 5c and 5d correspond to a sample annealed for 7 hours with the same meaning that 5a and 5b. As it can be observed, the same feature are found independent of the (annealing) sintering time, except that the degradation of the material is less important in the sample with the longer annealing time(, probably due to the fact that tangle of the grains with the larger aspect ratio avoid the movement of the glassy phase to the surface and the evaporation of the residual volatiles products).

(Fig. 5)

In order to check out if this damage is a consequence of the mechanical tests or to the experimental conditions, in some tests, another sample close to the tested one was placed. The ulterior microstructural characterization of these samples showed (Figure 6) the same feature

that the one deformed (Figure 6) indicating that the changes are due to the long exposure time that the samples are submitted at high temperature; in some experiments over 350 hours. The biggest porosity in the non tested samples indicates that the processes of deformation that takes place in the tested samples contribute to eliminate part of this porosity. For (these) the tests conditions, there are reactions between the sintering additives (Al_2O_3 and Y_2O_3) and the SiC grains[26-29], originating (producing) volatile(s) products as the ones indicated in the chemical reactions proposed in the literature[28-29].

$$SiC\ (s) + Al_2O_3\ (s) \longrightarrow Al_2O\ (g) + SiO\ (g) + CO\ (g) \qquad [2]$$

$$SiC\ (s) + Y_2O_3\ (s) \longrightarrow Y_2O\ (g) + SiO\ (g) + CO\ (g) \qquad [3]$$

(Fig. 6)

These processes induce a decomposition and elimination of a part of the SiC grains as well as of the sintering additives which are pull out to the surface where part of these products are deposed forming a rich layer in Y covering the SiC grains (Figure 7). The previous processes are responsible for the increase of porosity during the thermal treatment and of the decrease of intergranular phase. The biggest difficulty of eliminating the products of the reactions from the regions more far from the surface it makes that these processes are less important in the central areas of the sample The formed superficial layer (coating of the SiC grains close to the surface with Y,) together with the closed up of the cavities during the compression tests, produce a stability of the microstructure in such a way that after the first two or three days (few tenths ?? hours) of mechanical testing the microstructure remains unchanged as it can be observed in figure 2, where at the beginning of the test, there is a transient regime of approximately 4 % of deformation (between 2 and 3 days of deformation) before to get a steady state.

(Fig. 7)

After having reached the stationary state, the quantity of intergranular phase that remains and, therefore, the stable microstructure of the material depends on the temperature to that it has been subjected during the first days of the test in those that this stable microstructure is gotten, because the partial pressure of the gassy products that are obtained of the reduction of the Al_2O_3 and Y_2O_3 is strongly influenced by the temperature[29]. This influence of the temperature in the stable microstructure, is the responsible one that when carrying out a jump of temperature from T_1 to $T_2 > T_1$ in a tested sample at T_1 during a lingering time, the strain rates at T_2 is bigger that in another sample tested from the beginning to T_2, as corresponds to a sample with bigger quantity of intergranular phase[3]. This effect is shown in the figure 8. Nevertheless, the value of the creep parameters n and Q are independent of the temperature to that the material has reached the steady state, which it indicates that the mechanisms of creep are independent of the previous thermal history of the material, inside the limits of temperatures and stresses of our experiences.

(Fig. 8)

The SEM micrographs show that sintering time of the samples, in atmosphere of Ar, doesn't affect from a qualitative way to the processes that originate the structural changes of the material during deformation tests (Figure 5), except that the degradation of the material is less important in the sample with the longer sintering time. This is probably due to the fact that their microstructure of lengthened grains and intertwined avoid the movement of the

glassy phase to the surface and the elimination through her of the gassy products resultants of the reduction of the A_2O_3 and Y_2O_3.

4. Conclussions

*The microstructure characterization of the as-received samples showed a homogeneous distribution of the intergranular phase(s) and a density compared with the theoretical value of 98.8 % for samples sintered during (annealed) 1 hour and of 94.9 % for the longest time. The grain size increased from 0.64 to 1.61 μm when increasing the sintered time from 1 to 7 hours, taking place a very important elongating in a part of the grains. (, and the grains became ever more elongated as the sintering time increased from 1 to 7 hours.)

* For a same temperature and stress, the strain rate of the sample annealed 1 hour is at least one order of magnitude higher than for the sample annealed 7 hours. The different microstructure of the samples, with large grain size and aspect ratio developed during the longer sintered time can justified the biggest resistance to the deformation of the samples sintered during 7 hours.

* The almost unchanged morphology of the grains after deformation together with the values of the creep parameters: n between 2.4 and 4.5 for samples annealed 1 hour and between 1.2 and 2.4 for samples annealed 7 hours and Q around 700 $kJ.mol^{-1}$ regardless the experimental conditions, suggest that grain boundary sliding and the glide and climb of dislocation accommodated both by the bulk diffusion, can be two independent deformation mechanism operating in this liquid phase sintered SiC. The contribution of the activity of dislocations to the global process of deformation is more important when more high it is the applied tension and smaller the temperature.

* (Although there is degradation of the material due to) The existence of reactions in solid state between the sintering additives (Al_2O_3 and Y_2O_3) and the SiC grains producing volatiles products is responsible for the increase of porosity and of the decrease of intergranular phase in the samples during the thermal treatment to the test temperature. These effects are more important in regions near the surface that in the central area. (a)After few tenths hours of mechanical testing the microstructure remains unchanged as it can be observed in creep curves where steady states are perfectly defined. The sintering time of the samples doesn't affect from a qualitative way to this structural changes, except that the degradation of the material is less important in the sample with the longer sintering time

* Although the stable microstructure is influenced by the temperature of the sample until reaching the steady state, the value of the creep parameters n and Q are independent of this temperature, which it indicates that the mechanisms of creep are independent of the previous thermal history of the material, inside the limits of temperatures and stresses of our experiences.

Acknowledgements

The authors are grateful to Professors F. Guiberteau and A. L. Ortiz of the University of Extremadura for the preparation of the materials used in the work. The authors also thank the Ministry of Science and Technology for financial support through the project MAT2001-0799.

Referencias

[1] J. E. Lane, C. H. Carter, Jr. and R. F. Davis. “Kinetics and Mechanisms of high-temperature creep in silicon carbide: II, sintered α–SiC”. J. Am. Ceram. Soc., 71 (4), 281-295 (1988).

[2] R. D. Nixon and R. F. Davis. “Diffusion accommodated grain boundary sliding and dislocation glide in the creep of sintered alpha silicon carbide”. J. Am. Ceram. Soc., 75 (7), 1786-1795 (1992).

[3] M. Backhaus-Ricoult, N. Mozdzierz and P. Eveno. “Impurities in silicon carbide ceramics and their role during high temperature creep”. J. Phys. III. France, 3, 2189-2210 (1993).

[4] R. Hamminger, G. Grathwoht and F.Thuemmler. “Microanalytical investigation of sintered SiC Part I: Bulk material and inclusions”. J. Mater. Sci., 18, 353 (1983).

[5] Z.C. Jou and A.V. Virkar. “High temperature creep of SiC densified using a transient liquid phase”. J. Mater. Res., 6 (9), 1945-1949 (1991).

[6] A. Gallardo-López, A. Muñoz, J. Martínez-Fernández and A. Domínguez-Rodríguez. “High temperature compressive creep of liquid phase sintered silicon carbide”. Acta Mater., 47 (7), 2185-2195 (1999).

[7] C. H. Carter, Jr., R.F. Davis and J. Bentley. “Kinetics and Mechanisms of high-temperature creep in silicon carbide: I, Reaction bounded”. J. Am. Ceram. Soc 67 (10), 409-417 (1984).

[8] A. Muñoz, J. Martínez-Fernández, A. Domínguez-Rodríguez and M. Singh. “High-temperature Compressive Strength of Reaction-formed Silicon Carbide (RFSC) Ceramics”. J. Eur. Ceram. Soc., 18, 65-68 (1998).

[9] J. Martínez Fernández, A. Muñoz, A. R. Arellano López, F. M. Valera Feria, A. Domínguez Rodríguez and M. Singh. “Microstructure-mechanical properties correlation in siliconized silicon carbide ceramics”. Acta Mater., 51, 3259-3275 (2003).

[10] N. P. Padture. “In situ-toughened silicon carbide”. J. Am. Ceram. Soc., 77(2), 519-523 (1994).

[11] V. V. Pujar, R. P. Jensen and N. P. Padture. “Densification of liquid-phase-sintered silicon carbide”. J. Mater. Sci. Lett., 19[11], 1011-1014 (2000).

[12] H. Gervais, B. Pellissier and J. Castaing. “Machine de fluage pour essais en compression à hautes températures de matériaux céramiques”. Rev. Int. Htes Temp. et Refract., 15, 43-47 (1978).

[13] L. S. Sigl and H. J. Kleebe. “Core/rim structure of liquid phase-sintered silicon carbide”. J. Am. Ceram. Soc., 76, 773-776 (1993).

[14] A.L. Ortiz. “Control microestructural de cerámicos avanzados SiC sinterizados con fase líquida Y_2O_3 - Al_2O_3”. Tesis Doctoral, Universidad de Extremadura (2002).

[15] S. K. Lee and C. H. Lee. “Effects of α-SiC versus β-SiC starting powders on microstructure and fracture –toughness of SiC sintered with Al_2O_3-Y_2O_3 additives”. J. Am. Ceram. Soc., 77, 1655-1658 (1994).

[16] M. Nader, F. Aldinger and M. J. Hoffmann. “Influence of the α/β-SiC phase transformation on microstructural development and mechanical properties of liquid phase sintered silicon carbide”. J. Mater. Sci., 34, 1197-1204 (1999).

[17] Y. W. Kim, M. Mitomo and G. D. Zhan. “Mechanism of grain growth in liquid-phase-sintered β-SiC”. J. Mater. Res., 14, 4291-4293 (1999).

[18] H. Xu, T. Bhatia, S. A. Deshpande, N. P. Padture, A. L. Ortiz and F. L. Cumbrera. "Microstructural evolution in liquid-phase-sintered SiC: I, effect of starting SiC powder". J. Am. Ceram. Soc., 84, 1578-1584 (2001).

[19] M. H. Hon and R. F. Davis. "Self-diffusion of C-14 in polycrystalline β-SiC". J. Mater. Sci., 14, 2411-2421 (1979).

[20] M. H. Hon and R. F. Davis. "Self-diffusion of Carbon-14 in high purity and N-doped α-SiC single crystals". J. Am. Ceram. Soc., 63, 546-552 (1980).

[21] M. H. Hon, R. F. Davis and D. E. Newbury. "Self-diffusion of Si-30 in polycrystalline β-SiC". J. Mater. Sci. 15, 2073-2080 (1980).

[22] M. H. Hon, R. F. Davis and D. E. Newbury. "Self-diffusion of Silicon-30 in α-SiC single crystals". J. Mater. Sci., 16, 2485 (1981).

[23] M. F. Ashby, and R. A. Verrall. "Diffusional accommodated flow and superplasticity". Acta Metall., 21, 149-163 (1973).

[24] I. R. Spingarn and W. D. Nix. "Diffusional creep and diffusionallly accommodated grain rearrangement". Acta Metall., 26, 1389-1398 (1978).

[25] B. Walser and O. D. Sherby. "The structure dependence of power law creep". Scripta Metall., 16, 213-219 (1982).

[26] D. Sciti, S. Guicciardi and A. Bellosi. **"**Effect of annealing treatments on microstructure and mechanical properties of liquid-phase-sintered silicon carbide". J. Eur. Ceram. Soc., 21, 621-632 (2001).

[27] Tai-II Mah, K. A. Keller, S. Sambasivan and R. J. Kerans. "High-temperature environmental stability of the compounds in the Al_2O_3-Y_2O_3 system". J. Am. Ceram. Soc., 80, 874-878 (1997).

[28] T. Nagaro, H. Gu, G. D. Zhan and M. Mitomo. "Effect of atmosphere on supereplastic deformation behavior in nanocrystalline liquid-phase-sintered silicon carbide with Al_2O_3-Y_2O_3 additions". J. Mat. Sci., 37, 4419-4424 (2002).

[29] T. Grande, H. Sommerset, E. Hagen, K. Wiik y M. A. Einarsrud. "Effect of weight loss on liquid-phase-sintered silicon carbide". J. Am. Ceram. Soc., 80 (4), 1047-1052 (1997).

Figures captions

Figure 1: SEM micrographs of samples used in this work: (a) and (b) correspond to samples sintered during 1 hour, (c) and (d) correspond to samples sintered during 7 hours.

Figure 2: Strain rate versus strain in the creep test for a sample sintered in Ar atmosphere during 7 hours. In this plot the experimental conditions of the test and the calculated value of the creep parameters, n and Q, are indicated.

Figure 3: Strain rate versus applied stress for samples sintered in an Ar atmosphere for 1 hour. The temperature of the tests and the stress exponent obtained are indicated.

Figure 4: Strain rate versus applied stress for samples sintered in an Ar atmosphere for 7 hours. The temperature of the tests and the stress exponent obtained are indicated.

Figure 5: SEM micrographs of samples crept at 1625 ºC. (a) Correspond to a sample sintered for 1 hour and a region close to the surface and (b) to a region far from the surface. (c) Correspond to a sample sintered for 7 hours and a region close to the surface and (d) to a region far from the surface.

Figure 6: SEM micrographs of a sample sintered for 1 hour, subjected to the same thermal treatment that the deformed sample to 1625 ºC (Figs. 5a and 5b) but without exercising on her any stress: (a) region close to the surface and (b) region far from the surface.

Figure 7: (a) SEM micrographs of the surface in a sample sintered for 1 hour and crept at 1600 ºC. The presence of a layer covering the grains of SiC in the surface is observed. (b) EDS microanalysis of this layer.

Figure 8: Creep rate versus applied stress for samples sintered in an Ar atmosphere for 7 hours. The continuous lines correspond to a test with jumps of temperature between T_1 and T_2 and the discontinuous line correspond to a test to temperature T_2 from the beginning. The temperature of the tests and the stress exponent obtained are indicated.

Table 1: Values of the density and the morphological parameters measured before the mechanical tests, for both types of samples.

Process time (h)	Measured density ρ ($g \cdot cm^{-3}$)	Measured ρ/ theoretical ρ (%)	Diameter (μm)		Form factor		Aspect ratio	
			$\bar{d}$	σ_d	$\bar{F}$	σ_F	$\bar{F}_{asp}$	σ_{Fasp}
1	3.27 ± 0.02	98.8 ± 0.6	0.64 ± 0.02	0.29± 0.01	0.82 ± 0.01	0.11 ± 0.01	1.52 ± 0.02	0.34 ± 0.01
7	3.14 ± 0.03	94.9 ± 1.0	1.61 ± 0.05	0.99 ± 0.06	0.78 ± 0.01	0.12 ± 0.01	1.87 ± 0.04	0.66 ± 0.04

Table 2: Experimental conditions of the tests and values of the parameters n and Q obtained of the creep tests.

Process time (h)	T (ºC)	σ (MPa)	$\dot{\varepsilon}$ (s^{-1})	n	Q ($kJ \cdot mol^{-1}$)
1	1550	200-450	$4.2 \cdot 10^{-8}$-$1.5 \cdot 10^{-6}$	4.5 ± 0.2	685 ± 35
	1600	50-140	$6.3 \cdot 10^{-8}$-$7.1 \cdot 10^{-7}$	2.4 ± 0.1	
	1625	25-65	$9.6 \cdot 10^{-8}$-$7.4 \cdot 10^{-7}$	2.4 ± 0.1	
7	1580	210-400	$9.1 \cdot 10^{-8}$-$2.7 \cdot 10^{-7}$	2.4 ± 0.2	710 ± 90
	1600	160-320	$4.3 \cdot 10^{-8}$-$3.2 \cdot 10^{-7}$	2.4 ± 0.1	
	1625	60-200	$5.8 \cdot 10^{-8}$-$2.3 \cdot 10^{-7}$	1.2 ± 0.1	

Table 3: Summary of the experimental results obtained in previous works on the creep of the polycrystalline SiC fabricated with different techniques.

References	Characteristic of the material	Temperatures of the tests T (ºC)	Stresses of the tests σ (MPa)	Stress exponent n	Activation energy Q ($kJ \cdot mol^{-1}$)
Lane et al.[1]	α-SiC sintered to temperature of 2100 ºC. Additives: 0.5 wt % C, 0.42 wt % B and minor amounts (under 100 p. p. m.) of Fe, V, Se, Mg and Cu. Grain size d=3.7 μm.	1400-1800	138-414	1.44-1.71 (increases with T)	338-434 (T<1650 ºC) 802-914 (T>1650 ºC)
Nixon et al.[2]	α-SiC sintered to temperature of 2100 ºC. Additives: 0.5 wt % C, 0.42 wt % B and minor amounts (under 100 p. p. m.) of Fe, V, Se, Mg and Cu. Grain size d=3.5, 4.9 y 7.5 μm.	1500-1750	35-373	1.1-1.4 (T<1650 ºC) 1.4-2.5 (T>1650 ºC) (increases with d)	387-541 (T<1650 ºC) 838-877 (T>1650 ºC) (decreases with d)
Backhaus-Ricoult et al.[3]	SiC obtained by hot isostatic press (HIP) to temperature of 2000 ºC and pressure of 2 kbar. (a) without impurities and with grain size d=0.5 μm. (b) with impurities of B, Si, Fe, O and C (below 2000 p.p.m.) and grain size d=3.5 μm.	1500-1700	100-1100	1.5 (σ<500 MPa) 3.5-4.0 (σ>500 MPa)	(a) 364 (σ<500 MPa) (b) 453 (σ<500 MPa) 629 (σ>500 MPa)
Hamminger et al.[4]	SiC doped with Al and C and with B and C.	1470-1660	100-190	~1	796
Jou et al.[5]	SiC sintered with liquid phase (LPS) of Al_2OC (10 %-wt) to temperature of 1875 ºC. Grain size d=2 μm.	1500-1650	38-200	1.74	743

Gallardo-López et al.[6]	6H-SiC sintered with liquid phase (LPS) of Y_2O_3 and Al_2O_3 (less than 2 %-vol). Grain size d=1.2 μm.	1575-1700	90-500	1.6	840
Carter et al.[7]	SiC obtained by reaction of the Si in gassy state with a porous preform of SiC with free C (RBSC). Final content of free Si: between 10 and 12 %-vol.	1575-1650	110-220	5.7	711

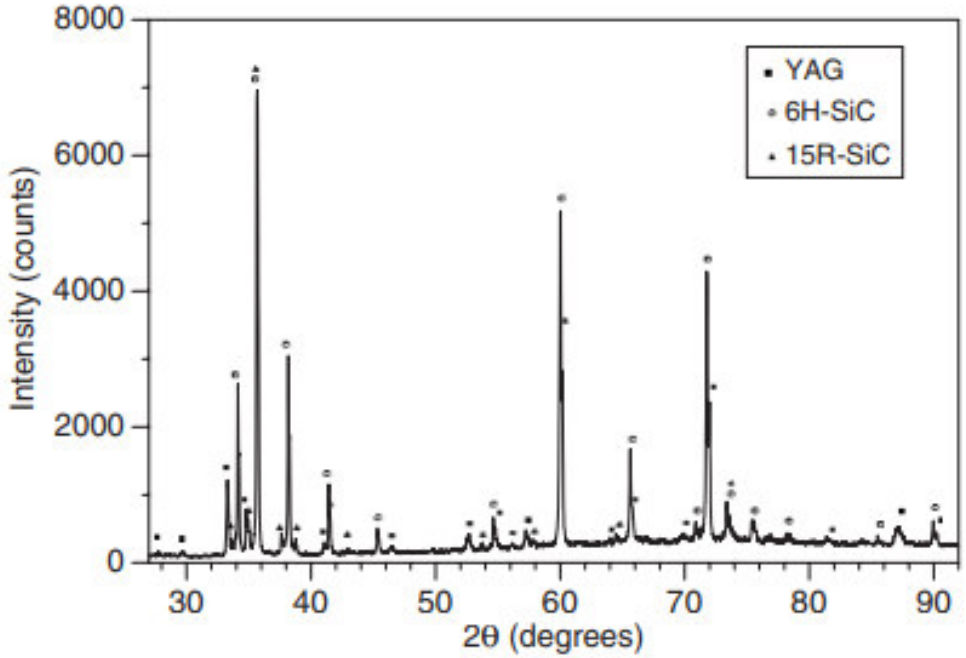
8000
6000
4000
2000
0
Intensity (counts)
30
40
50
60
70
80
90
2θ (degrees)
YAG
6H-SiC
15R-SiC

Figure 1

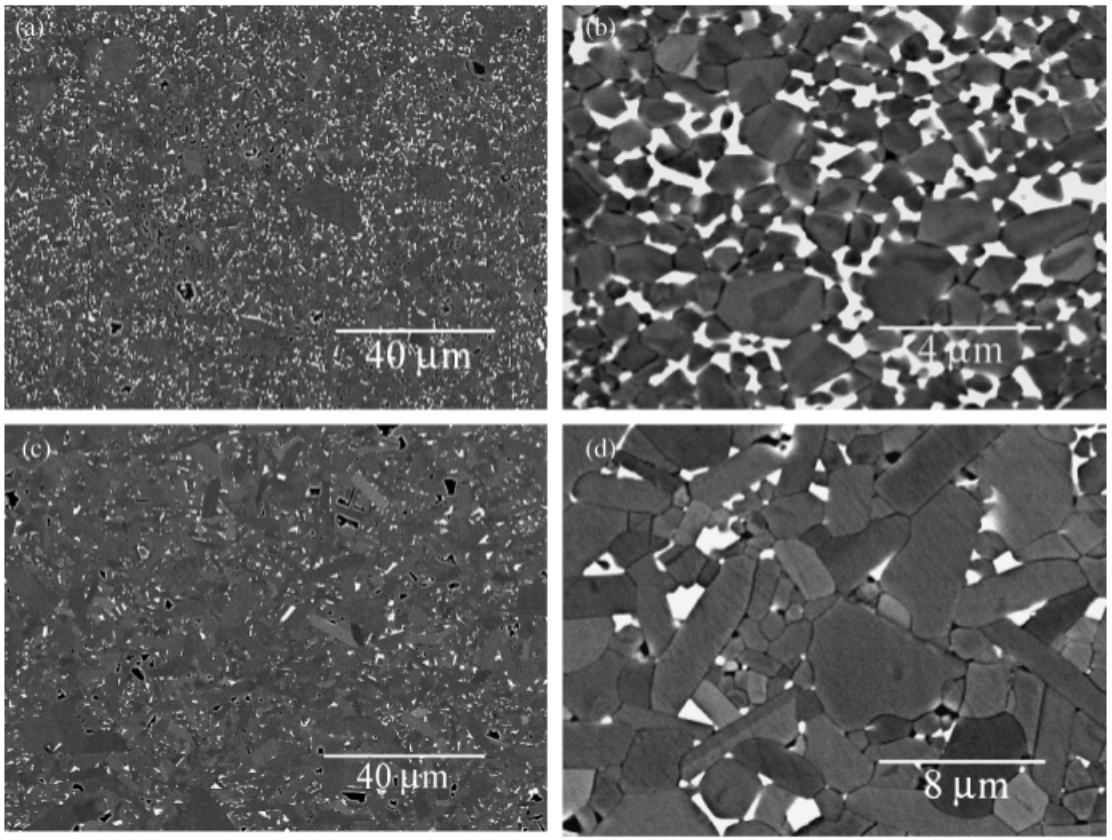

Figure 2

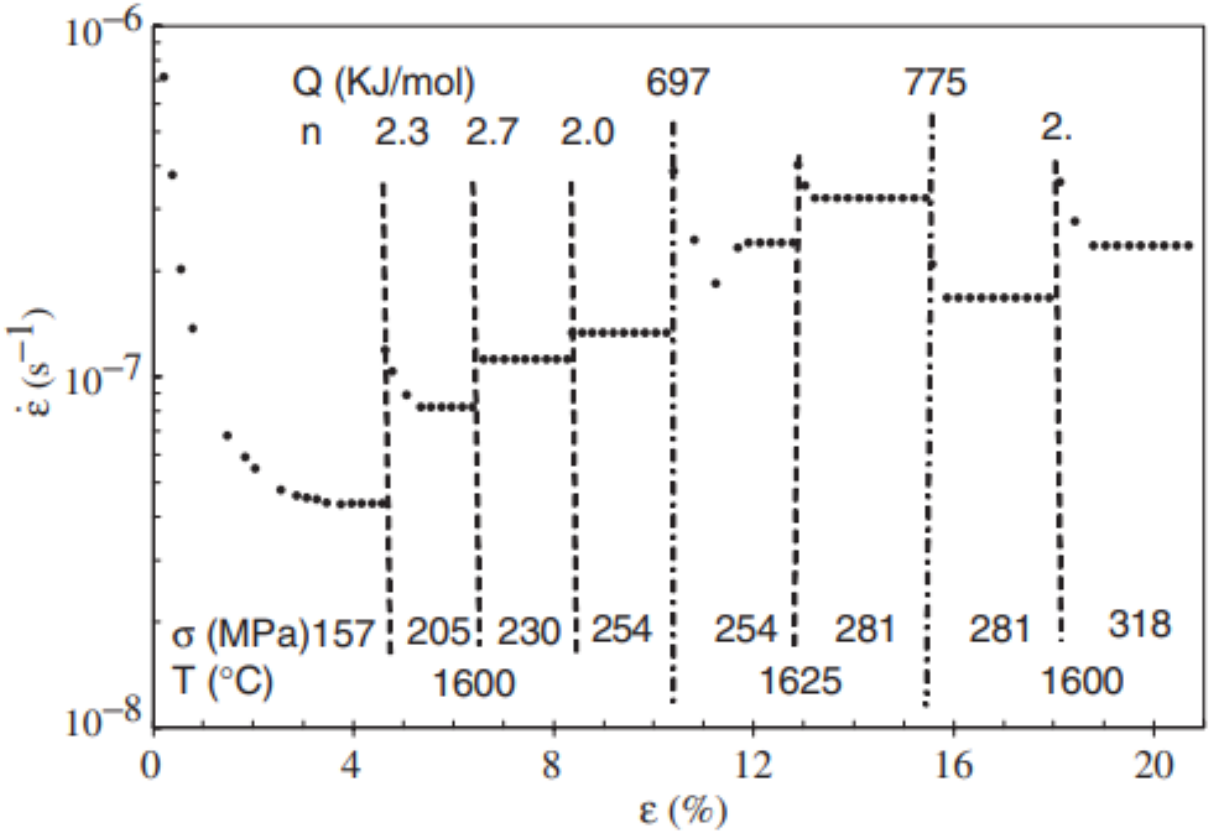
Q (KJ/mol)
697
775
n
2.3
2.7
2.0
2.
σ (MPa)157
205
230
254
254
281
281
318
T (°C)
1600
1625
1600
10^{-6}
10^{-7}
10^{-8}
$\dot{\varepsilon}$ (s^{-1})
0
4
8
12
16
20
ε (%)

Figure 3

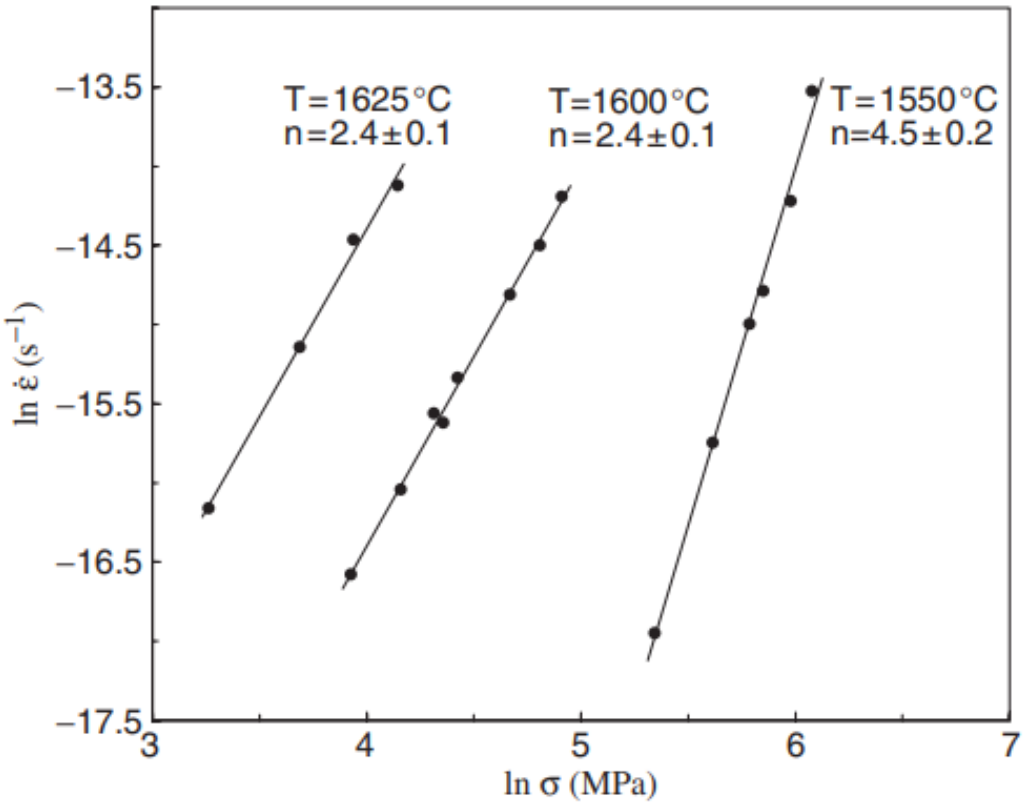
T=1625°C
n=2.4±0.1
T=1600°C
n=2.4±0.1
T=1550°C
n=4.5±0.2
−13.5
−14.5
−15.5
−16.5
−17.5
3
4
5
6
7
ln ε̇ (s⁻¹)
ln σ (MPa)

Figure 4

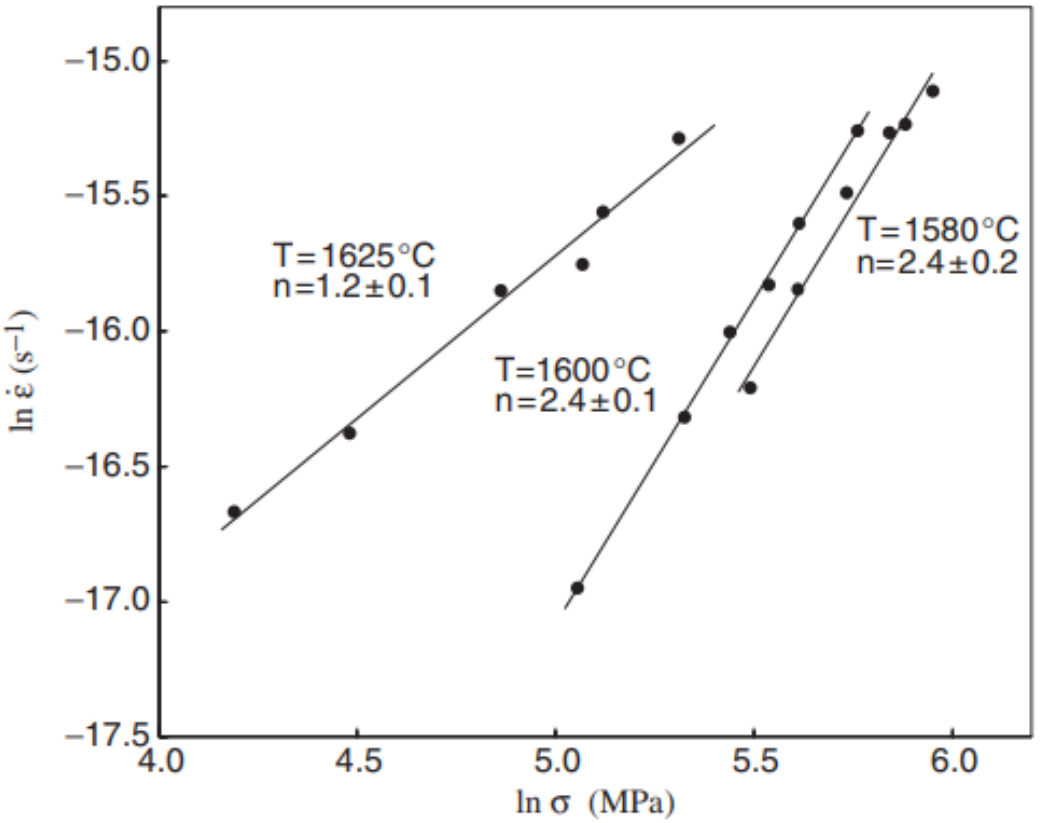
−15.0
−15.5
−16.0
−16.5
−17.0
−17.5
4.0
4.5
5.0
5.5
6.0
ln ε̇ (s⁻¹)
ln σ (MPa)
T=1625°C
n=1.2±0.1
T=1600°C
n=2.4±0.1
T=1580°C
n=2.4±0.2

Figure 5

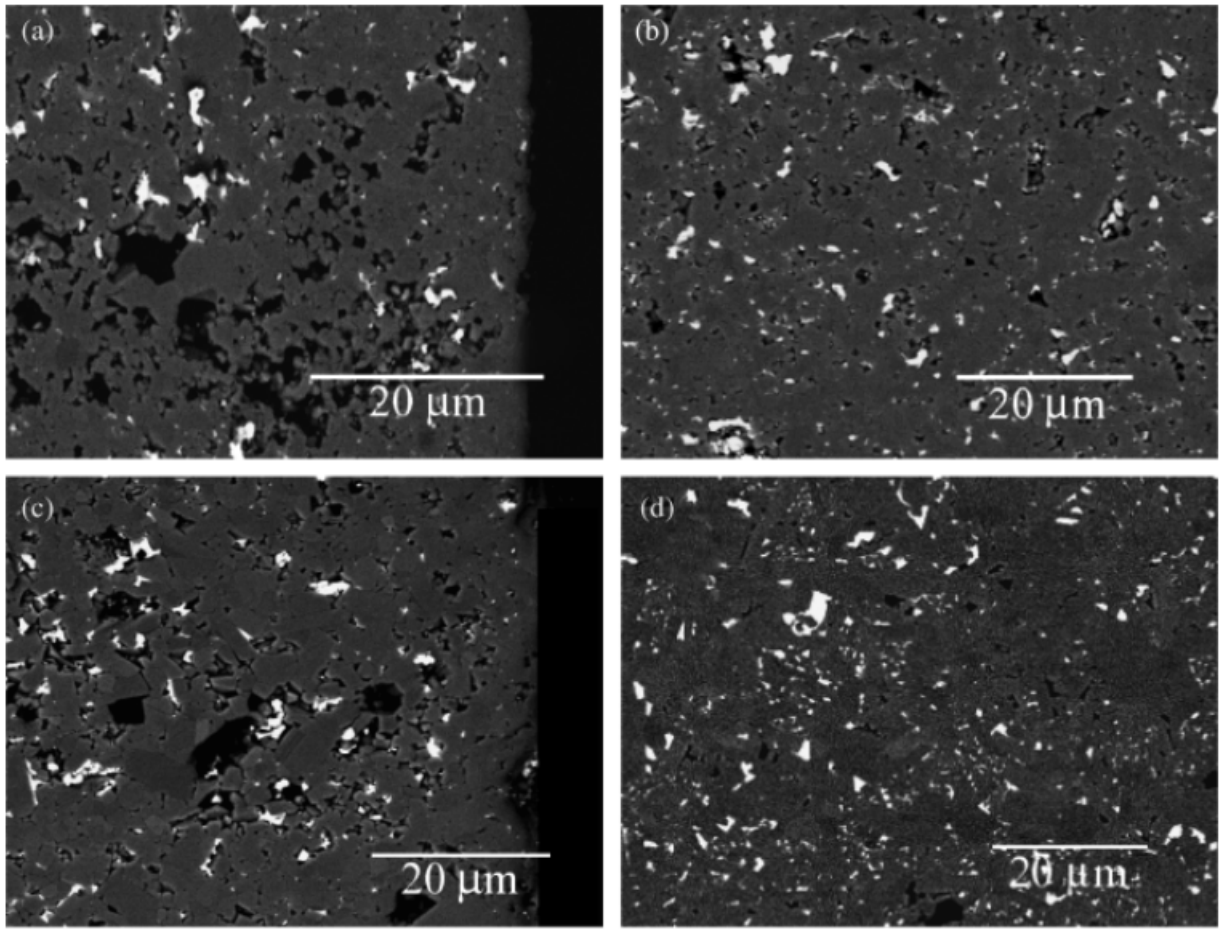

Figure 6

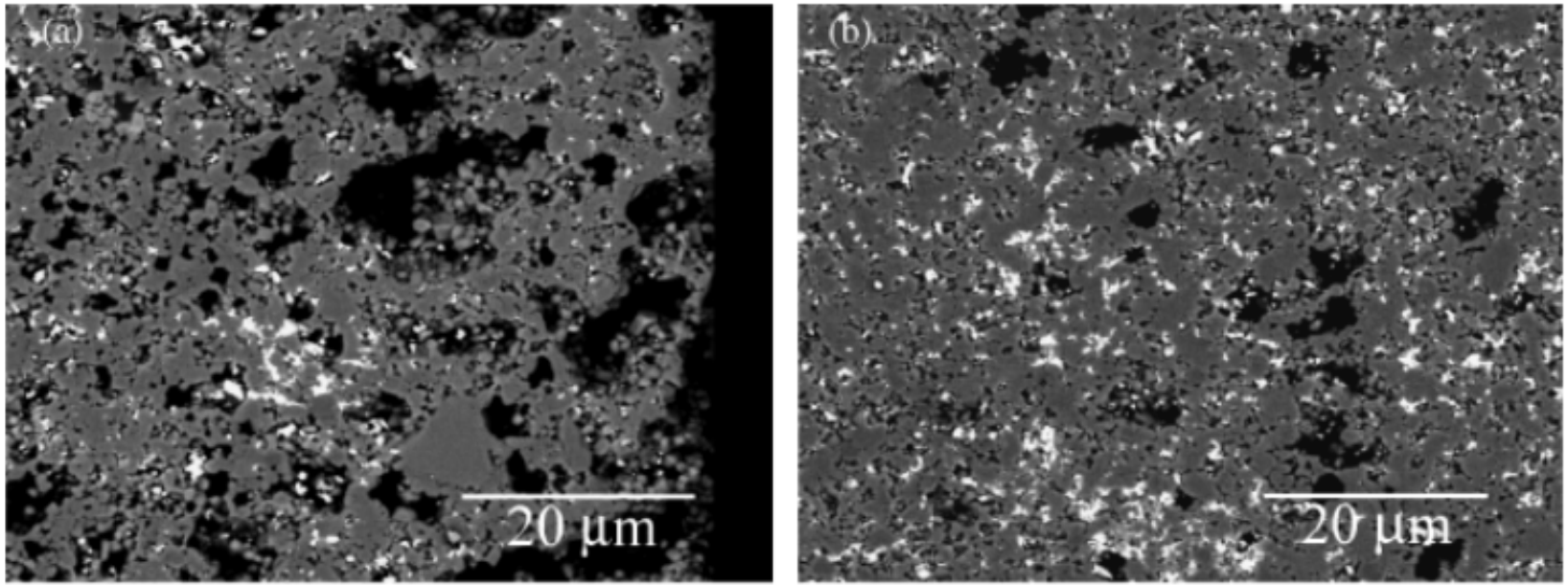

Figure 7

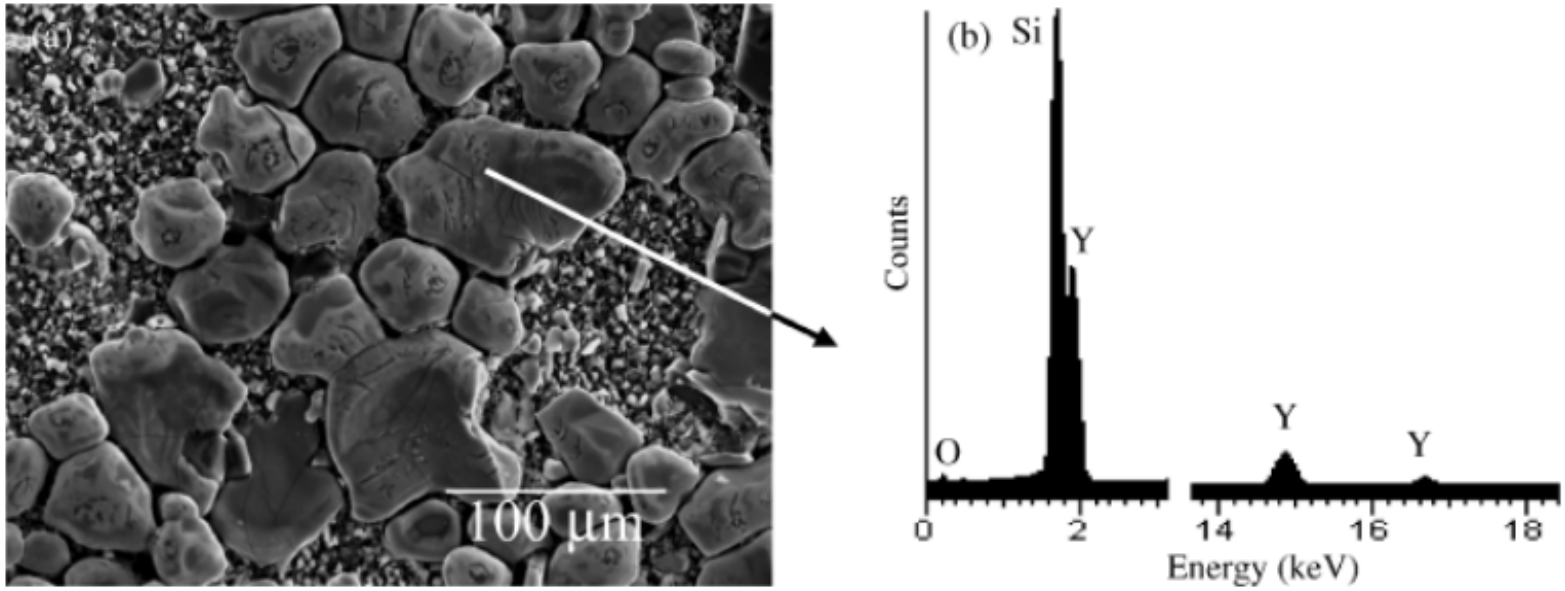

Figure 8